International Journal of Sustainable Applied Sciences (IJSAS)
Vol. 3, No. 4, 2025: 235-248

Organic Preparation of Graphene Nano Foil Derivatives and Membranes and Study of some of Their Applied Properties

Tareq Bandar Mahmood
Ministry of Education the General Directorate of Education in Salah Al-Deen
Corresponding Author: Tareq Bandar Mahmood tareqaldori1974@gmaill.com

A R T I C L E I N F O

Keywords: Organic Preparation, Graphene, Nano Foil, Derivatives, Membranes, Applied Properties

Received : 19, February
Revised : 20, March
Accepted: 30, April

©2025 Mahmood: This is an open-access article distributed under the terms of the Creative Commons Atribusi 4.0 Internasional.

A B S T R A C T

In this study, nanoscale graphene oxide was prepared using a modified Hummer method. The phenolic compound was prepared through diazonium salt reactions, which occurred between the diazonium salt of para-aminophenol and silica gel, forming a 4-silica gel-phenol complex. Graphene oxide was decorated with a 4-silica gel-phenol composite after being convert into the sodium salt of the phenolic compound. This composite was usage in the preparation of cement mortar. When mixed with the cement mortar, it achieved high compressive strength, demonstrating the strong impact of the prepared composite and is beneficial when mixed with cement mortar and demonstrated good results.

DOI: https://doi.org/10.59890/ijsas.v3i4.34
ISSN-E: 3025-5597
https://dmimultitechpublisher.my.id/index.php/ijsas

INTRODUCTION

Graphene possesses excellent physical, mechanical, chemical, thermal, and visual possessions that proposal marvelous potential for requests in numerous subdivisions (1). It is a dense atomic piece of carbon atoms composed of hexagonal lattice pieces. Graphene-based carbon is recognized as the lightest and strongest material. The profound request of graphene is attributed to its high surface area, chemical stability, and electrical properties (2). Graphene has arose as a star carbon nanomaterial owing to its excellent motorized, electrical, and thermal possessions (3). In a study by Gong et al., it was exposed that the introduction of 0.03 wt.% graphene oxide sheet into adhesive grout can upsurge the compressive and tensile forte of the cement complex by additional than 40% owing to the reduced pore structure of the cement paste. Furthermore, the presence of GO sheet improves the hydration of the cement paste (4).

LITERATURE REVIEW

Graphene, since its discovery in 2004, has become a very promising material due to its unique two-dimensional structure and extraordinary properties such as high thermal and electrical conductivity, mechanical strength, and optical sealing. One of the major challenges in its widespread use is an efficient, environmentally friendly, and high-quality synthesis method.

Several methods have been developed to produce graphene, such as mechanical exfoliation, chemical vapor deposition (CVD), reduction of graphite oxide, and electrochemical techniques. However, each of these methods has limitations both in terms of production scale, process complexity, cost, and environmental impact. In particular, organic solvent-based methods often produce graphene with low structural quality or small size.

This article discusses an innovative organic approach-based graphene synthesis method utilizing organic solvents and a cleaner reaction system. This approach is called "organic preparation of graphene nanofoils," which aims to produce graphene with a thin foil (nanofoil) structure, large lateral size, and high crystalline quality without metal contamination or oxidation residues.

In the relevant literature, chemical approaches such as reduction of graphene oxide using reducing agents (e.g., hydrazine or ascorbic acid) produce graphene with structural defects. Organic liquid exfoliation methods have also been explored, but their efficiency is still low due to the lack of interaction between the solvent and the graphite layer. This paper addresses these challenges by proposing an approach that combines the advantages of both exfoliation and chemical methods, but with better reaction control and a more stable reaction environment. Overall, this organic approach has the potential to be a more environmentally friendly and economical alternative for the production of high-quality graphene. Previous literature provides a strong basis that improvements in the control of synthesis parameters and the selection of reaction media can significantly affect the final quality of graphene. This paper strengthens this understanding with experimental evidence and in-depth characterization.

METHODOLOGY

Preparation of Graphene Oxide (GO) using the Hammer Method:

Place a 1000 ml beaker in an ice immersion and add 23 ml of focused sulfuric acid under magnetic rousing. 0.75 g of sodium nitrate was then additional. After 15 minutes, 0.5 g of graphite was additional to the mixture and stirred gradually for 10 minutes. 3 g of potassium permanganate was then add to the mixture slowly over 10 minutes, while maintaining the temperature below 10°C.

The mixture was then left in the ice bath for 5 minutes. The mixture was then remove from the ice bath and allowed to be stirred attractively for 1.5 hours. 23 ml of purified water was then gradually added drop by drop over 20 minutes. The temperature was then increased to 98°C for 20 minutes. 70 ml of warm purified water (50°C) was then add and allow to stir for 10 minutes at room temperature. 7.5 ml of hydrogen peroxide (30%) was then add and allow to stir for 30 minutes. 150 ml of distill water was then additional and the mixture was allowed to stand for 24 hours, as shown in Figure 2-2. The mixture was poured and collected once, and the precipitate was washed once with a 10% hydrochloric acid solution, followed by five washes with deionized water until the pH reached 7. 2_ Preparation of the Compound: Preparation of the Silica Salt

Step 1: Preparation of the Silica Salt

Place 1 g of highly porous silica gel in a suitable beaker containing a 10% sodium hydroxide solution. Heat the mixture to 60 °C for 10-5 minutes, then dry and filter.

Step 2: Preparation of the Diazonium Salt

Diazonium salt was prepared by adding 1 g (0.01 mol) of para-hydroxyaniline to a beaker containing a 1:1 solution of (water:concentrated hydrochloric acid) cooled using an ice bath at 5 °C. M, and dissolve in another beaker 0.6 g (0.01 mol) of sodium nitrite in the minimum quantity of distill water sufficient for dissolution. Add the second beaker to the first beaker gradually over 5 minutes with cooling and continuous stirring.

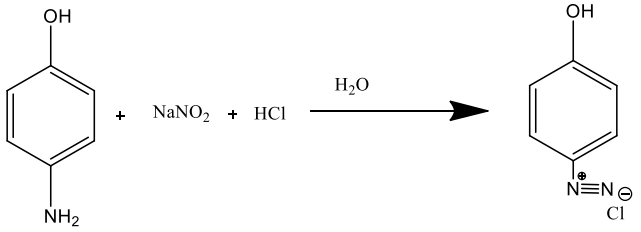

Figure 1. Preparation of the Diazonium Salt

Step 3: Prepare 4-silica gel-phenol by adding the ingredients of step 2 to step 1, stirring for 10-15 minutes at room temperature until the color of the mixture stabilizes. Then filter, wash with distill water, and dry at 60°C (5).

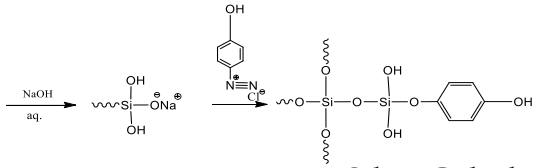

Figure 2. Prepare 4-Silica Gel-Phenol

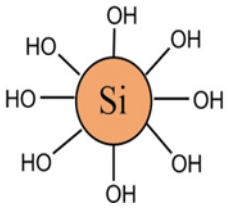

Figure 3. Preparation of Sodium Phenoxide for Silica Gel-Phenol

Step Four: Preparation of Sodium Phenoxide for Silica Gel-Phenol

Place 1 g of aromatic silica gel derivatives in a suitable beaker containing a 10% sodium hydroxide solution. Heat the mixture to 60°C for 5-10 minutes, then filter and dry.

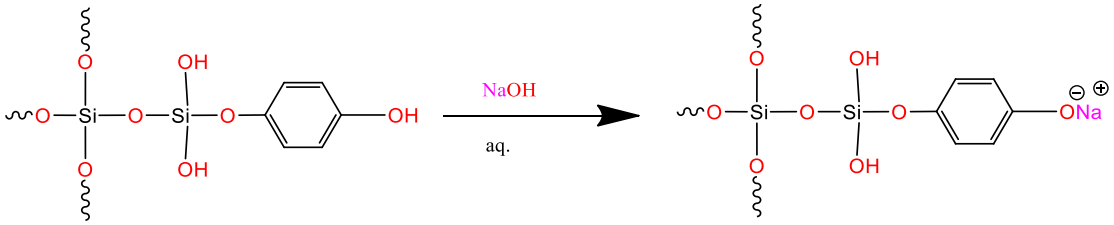

Figure 4. Preparation of the Aromatic Silica Gel Derivative with Graphene Oxide

Step Five: Preparation of the Aromatic Silica Gel Derivative with Graphene Oxide:

0.1 g of the ready graphene oxide was additional to 50 ml of distilled water. The solution was homogenized using ultrasound. The graphene oxide solution was additional dropwise to the Aromatic Silica Gel Derivative Solution for 10 minutes. The resulting mixture was poured and filtered with distilled water and dried at 60°C (6).

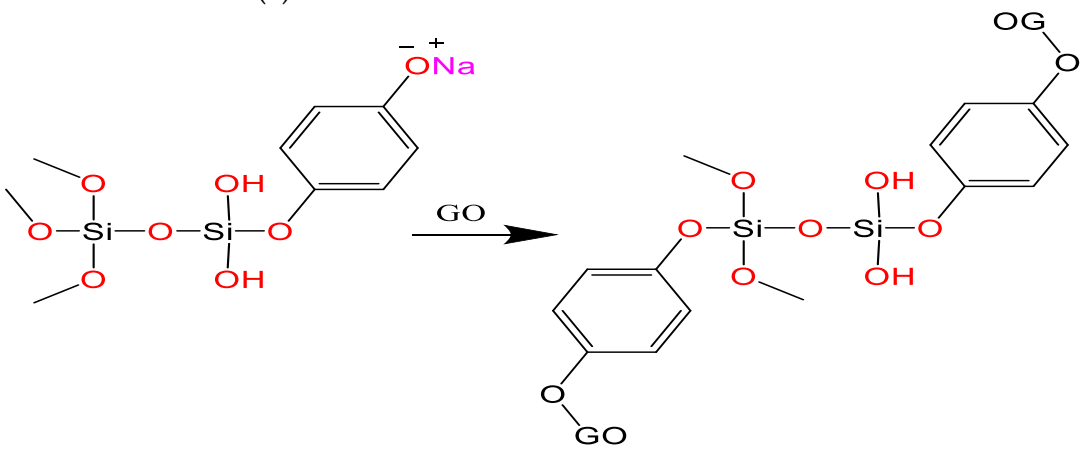

Figure 5. Resulting Mixture was Poured and Filtered with Distilled Water and Dried at 60^0C

Practical Application

The nanocomposite was varied with water free of organic compounds and stirred and impurities magnetically for 2 minutes. It was then moved to a sonication expedient for 90 minutes. The composite was then moved to a mixer and mix by normal Portland cement and natural sand. A 0.5% plasticizer by weight was added to all mixtures for four minutes. After mixing, the mixture was transferred to cubes gauging 50 mm x 50 mm x 50 mm. The cubes were greased with oil and the combination was decanted in to the cubes usage a

vibrator. The cubes were then left to stand for 24 hours. The cubes were then detached from the molds and place in a water bath (7).

RESULT AND DISCUSSION

Elaboration and Description of Graphene Oxide Nanofilaments

The elaboration of graphene oxide involves the oxidation step represent by the Hummer reaction, where carboxyl, epoxy, hydroxyl, and ketone carbonyl groups are formative at the edges of the exfoliated sheets and at their internal edges at cracks, as shown in the next equation:

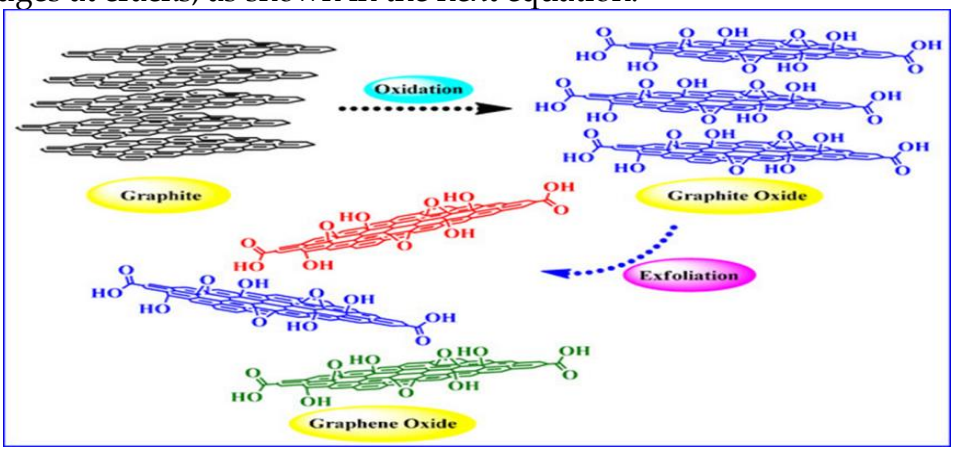

Figure 6. Elaboration and Description of Graphene Oxide Nanofilaments

The ultraviolet spectrum of graphene oxide nanosheets displayed a distinctive and broad band due to the overlapping alcoholic and carboxylic hydroxyl groups (OH) at cm-1 (3392). The measure too displayed a band at cm-1 (1622) due to the stretching of the C=C double bond. The measurement also showed two bands at cm-1 (1730, 1225), which are the other distinctive bands due to the stretching of (C=O, C-O) in the carboxyl group, respectively. The graphene oxide sheets cover epoxy group signified by stretching (C-O). These groups give bands at the range (1225, 1064) which appear broad and partially overlap with a winding band. The (OH) group displays a broad band partly meeting with a winding band at cm-1 (1506). The appearance of the two bands designates the attendance of soaked aliphatic groups e.g. (CH2) subsequent from The tautomerism that stretches certain terminal acetyl group, which is reinforced by the apparent pure vCH)) in addendum to the existence of asymmetric and symmetric vibration in the field cm-1 (2983.32, 2830.05) due to the (C-H) group, too abundant curvature and stretching feelings of the (C-H) group manifested in the field cm-1 (900-400) (8).

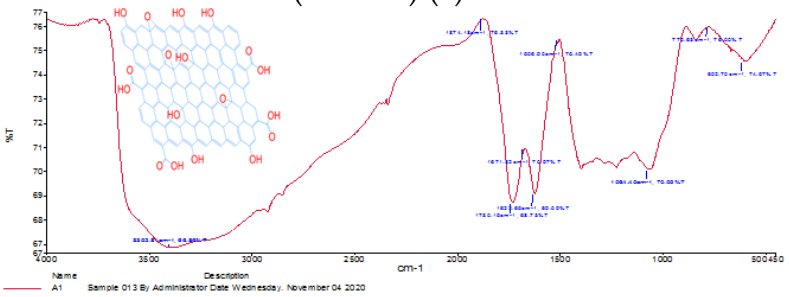

Figure 7. The Appearance of the Two Bands Designates the Attendance of Soaked Aliphatic Groups

XRD for studying the crystal structure of graphene oxide (GO) displayed angle values of 12.35, 12.59 and 11.10 = 2θ degrees identical to the Miller index (100) by the dimension among the layers of d = 7.15 A˚, which was greater than that of graphite, where d = 0.33 nm. The upsurge in the dimension among the layers is attributed to the space amid them resulting from the oxidation of the edges and the middle of the graphite sheets, which clues to increased flaking and separation of the layers.

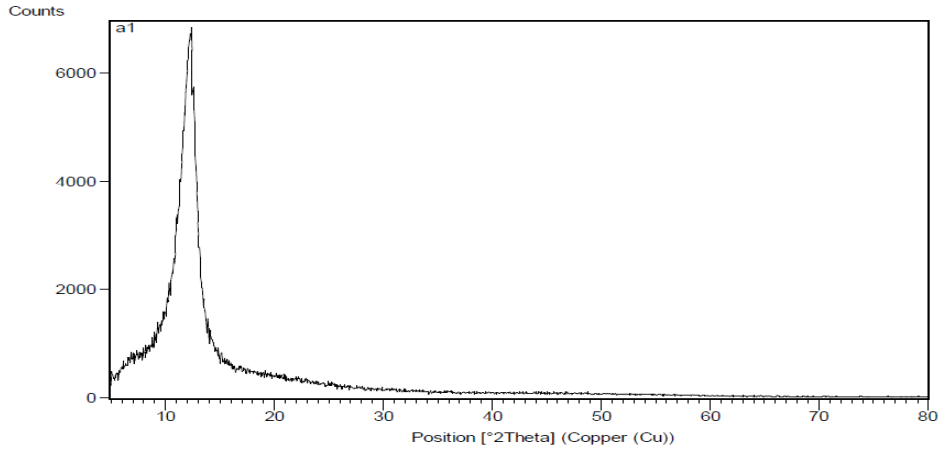

Figure 8. The Upsurge in the Dimension among the Layers is Attributed

Observing the morphological imageries of complex A1 clearly reveals the extent of peeling result from oxidation, as seen in the space among the sheet clusters (layers) within sample (a), as well as the nanoscale thicken of each layer. Image (b) also presented the attendance of wide sheets covering nanoscale blows with distinct edges, with clear oxidation in the form of thickening on the edge of these crack or in the method of oxidized carbon grain measure nanometers. These cracks might be attribute to the lack of transparency of the sheets, as well as their aloft susceptibility to doping with compounds and their involvement in numerous beautifying responses on the surface of the sheets as well as their edge (9). The aloft tortuosity of the nanosheets, as in image (c), designates a competition with the little number of sheets, which stretches them suppleness. The sheet thick was 40 nm, with clear surface unevenness, as the sheets were nearly vertical at certain point. Figure (3-3) displays SEM images of compound A1.

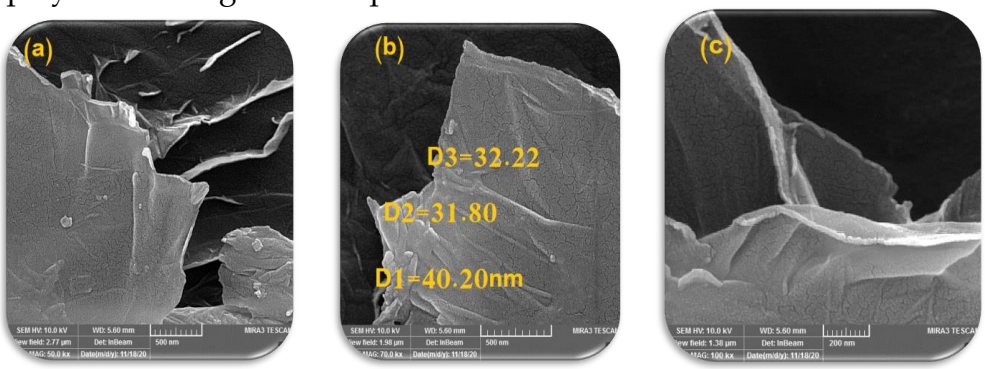

Figure 9. Display SEM Images of Compound A1

From the perpendicularity value shown in the SEM image (a) for pattern A1, we letter that the value assumed by the AFM dimension for the tallness of the taster surface as in (a1) of the AFM image, as well as figure (), which pattern values of 16.5 nm and 6.0 nm, are not undistinguishable. This designates the change in the pattern topography and the heterogeneity of the surface. This is reliable with the diverse peeling potentials of the areas on the graphite surface, as the figure displays the diverse detachments among the lowest and the top (Top, both) for the top of 100 nm of the pattern designated for imaging with dimension of 200 * 200 nm. The high peak of the variance among the low bottom and the high peak was 16.5 nm, as in Figures (3-5) and (3-6). This designates the unevenness present in the surface and give an idea of the large amount of void in the layer, which makes it have a large surface space of 24% of the upsurge ended 100% present in the surface.

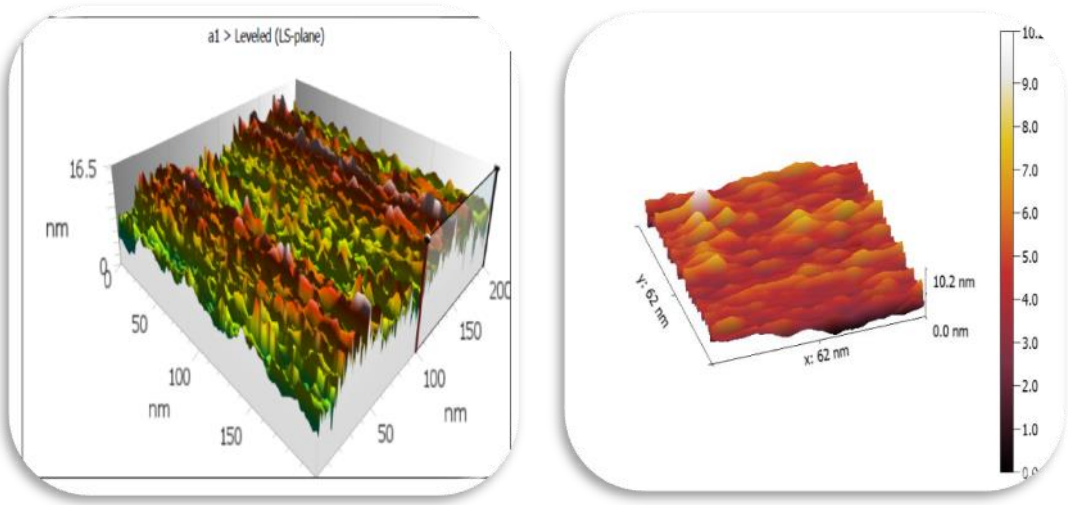

Figure 10. Which Pattern Values of 16.5 Nm And 6.0 Nm, are not Undistinguishable

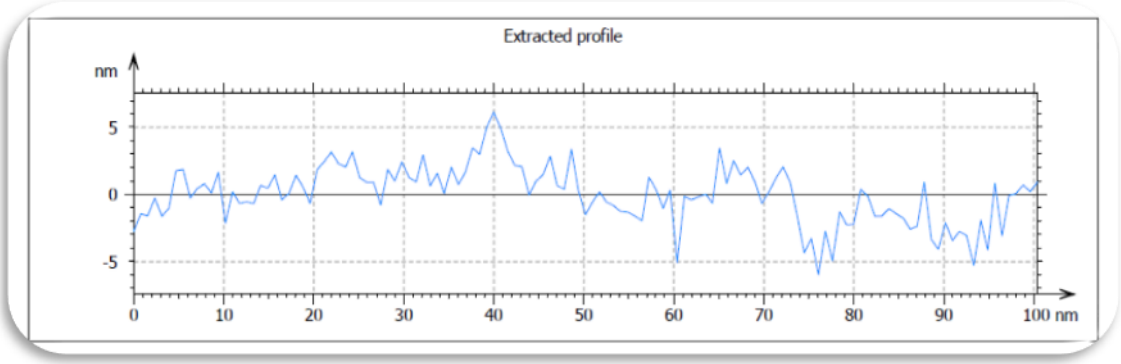

Figure 11. Extracted Profile

Discussion of the electrochemical preparation of tetraphenyl 4,4-diol:

The FT-IR spectrum of the complex shows clear value for the aromatic ring at the stretching of the (v C=C) bond in the range (1568-1645) cm-1 and (v Si–O), respectively, and the stretching band of (v C–O) in the range (1051-1064) cm-1, (v OH) in the range 3400 cm-1, and (A r (v C–H) in the range 3030 cm-1. Figure (3-27) shows the infrared spectrum of the aromatic silica gel derivative.

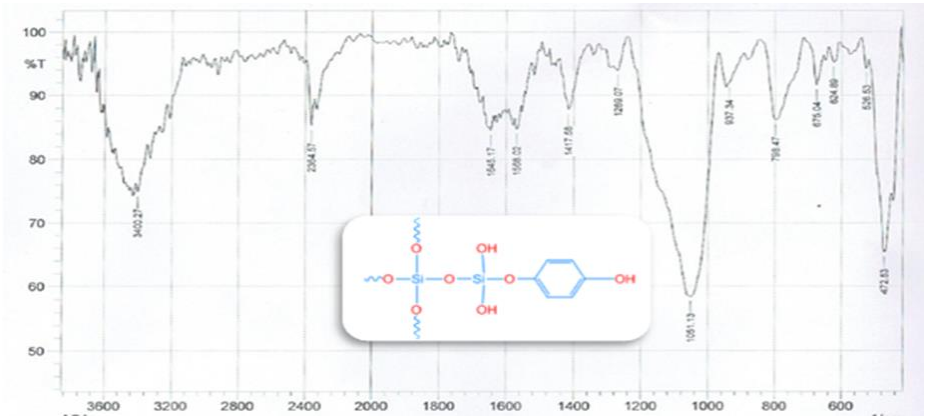

Figure 12. Shows the Infrared Spectrum of the Aromatic Silica Gel Derivative

The ultraviolet spectrum of the nanocomposites (A5) show value indicating the presence of aromatic character in the structure in the range (1431-1519) cm-1, which is attribute to the aromatic (v C = C) widening, and at (1035-1076) cm-1, which are due to the widening of the Si-O and Si-OH bonds, individually, as well as a clear band at (~1100) cm-1, which is credited to the widening of Si-O-Si.

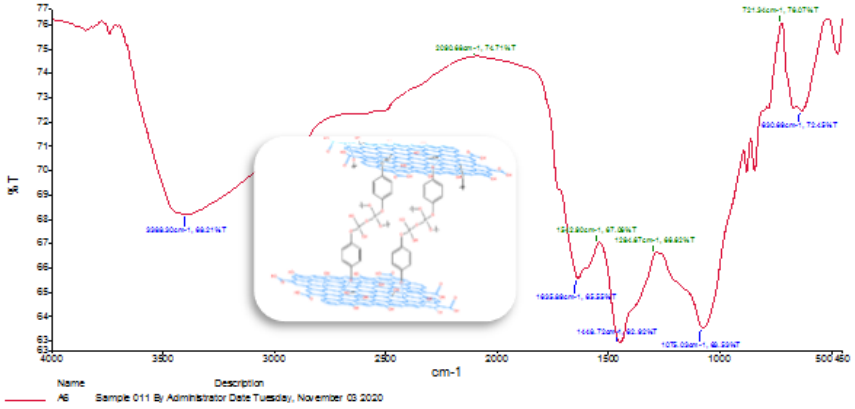

Figure 13. Which is Credited to the Widening of Si-O-Si.

Discussion of the ultraviolet spectrum of the A5 (Si GO) complex:

The infrared range of the A5 nanocomposites, as shown in Figures (3-28) to (3-31), showed values indicating the presence of aromatic properties in the structure in the range (1431-1519) cm-1, which is credited to the aromatic (v C = C) widening, and at (1035-1076) cm-1, which are credited to the widening of the Si-O and Si-OH bond, individually. There is also a clear band at (~1100) cm-1, which is credited to the widening of Si-O-Si (10). XRD Discussion of Complex A5 (Si GO). The X-ray spectrum of Complex A5 (Si GO) show diverse 2θ angle values than that of graphene oxide (A1 GO). The 2θ peak was 32.495, the interlayer spacing was d = 2.64 ˚, the grain size was D = 10.72, and the number of layers was n = 3.83.

The XRD pattern shows the presence of multiple crystalline forms in the sandwich-like sample, but this process was accompanied by a high degree of exfoliation of the sample, resulting in a grain size lower than the closely spaced layers of the parent compound A1 (with a clear change in the SEM images). This indicates the occurrence of additional exfoliation of the layers, which may

be attributed to the substitution of silicon atoms. It consists of five main crystalline types expected in the XRD spectrum. Figure (3-32) shows the XRD spectrum of Compound 5A.

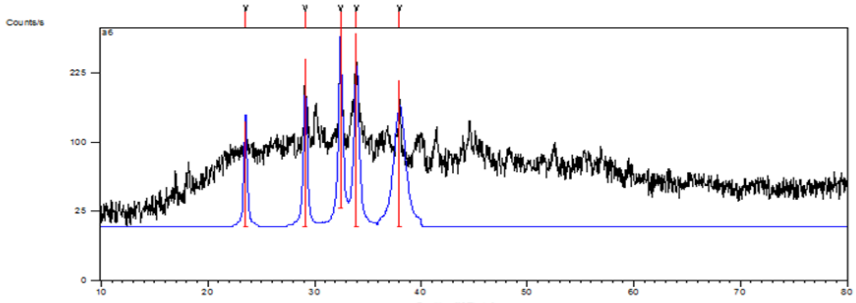

Figure 14. Shows the XRD Spectrum of Compound 5A

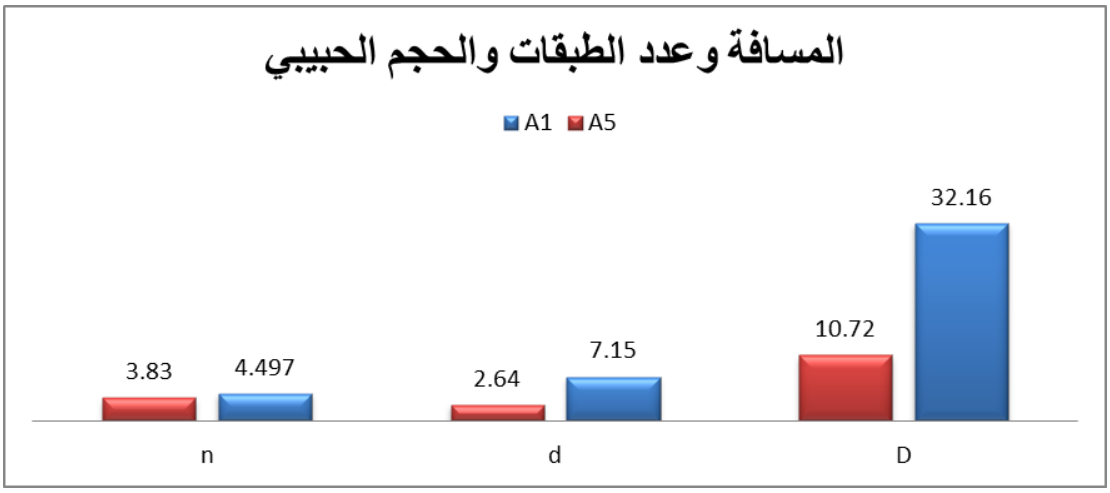

Figure 15. Shows the XRD Spectrum of Compound 5A

Discussion of SEM results for composite A5 (Si GO)

The scanning electron microscope (SEM) morphological images of sample A6 showed a high degree of regularity in the stripe patterns of the exfoliation, which suggests an important upsurge in surface area (a) and the presence of diffusion of the decoration on the surface (b). Also observed were:

1. The attendance of crack at a lower rate compared to non-silicon composites (c), as shown in Table 3-13.
2. The presence of more regular aggregates of the decoration material on the edges of the stripe-patterned sheets, with diffusion on the surface of the sheets (c). This difference from previous decorations may be attributed to the fact that it was decorated using the SN2 mechanism rather than the SN1 Ar Rad mechanism. This resulted in the failure to maintain the shape of the carbon sheets over their entire area, but rather increased their exfoliation and convergence, as shown in the XRD peaks. Figure (d) also shows the beginning of the growth of these sheets. (3) The decoration on the rings gave an average width of 11.70 nm, as shown in Table (3-14), image (f). Figure (3-36) shows SEM images of compound 5A.

Figure 16. Shows SEM Images of Compound 5A

AFM Discussion of Compound A5 (Si GO)

The AFM image of complex A5 show a high roughness of 69.72, which is higher than all the electromechanical derivatives A4-A2, which ranged between 19.81 and 62.4 nm. This supports the SEM images, which showed increased exfoliation due to the effect of spontaneous silicon dimerization between the plates. Figure (3-37) shows the AFM images of compound A5, showing the surface roughness. Figure (3-38) shows the selective curve of compound A5. Figure (3-39) shows the AFM images of compound A5.

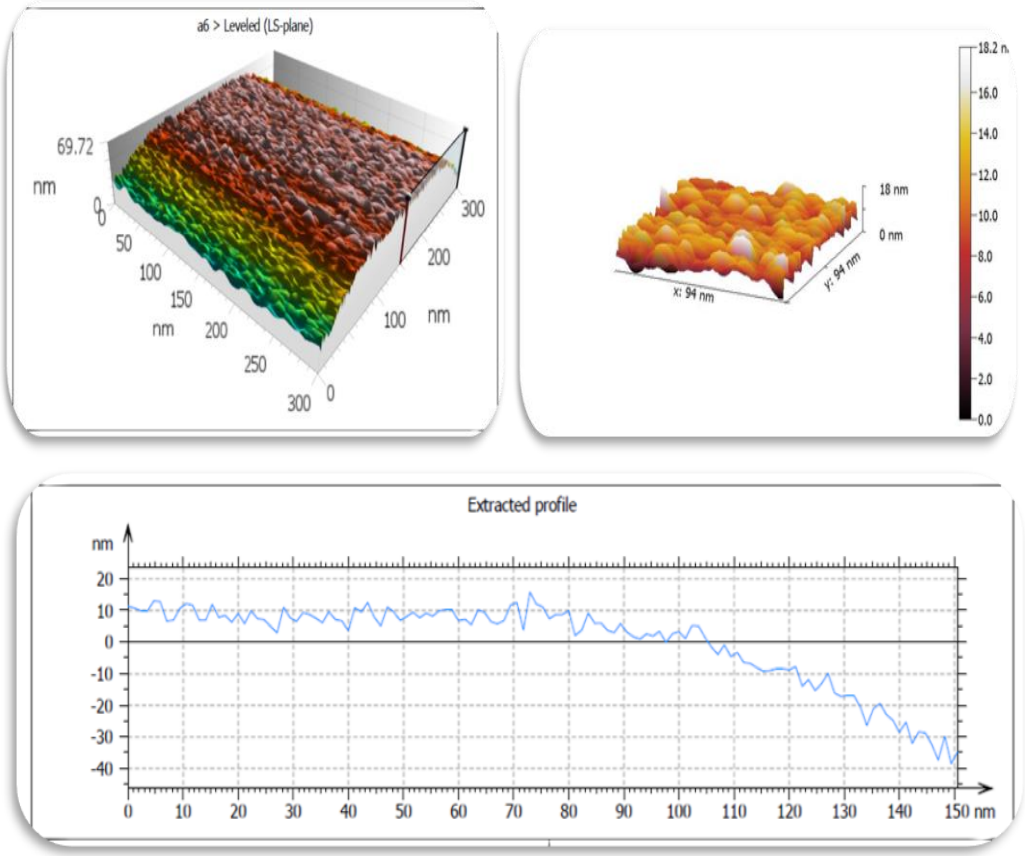

Figure 17. Shows the AFM Images of Compound A5

Discussion of the applied part:

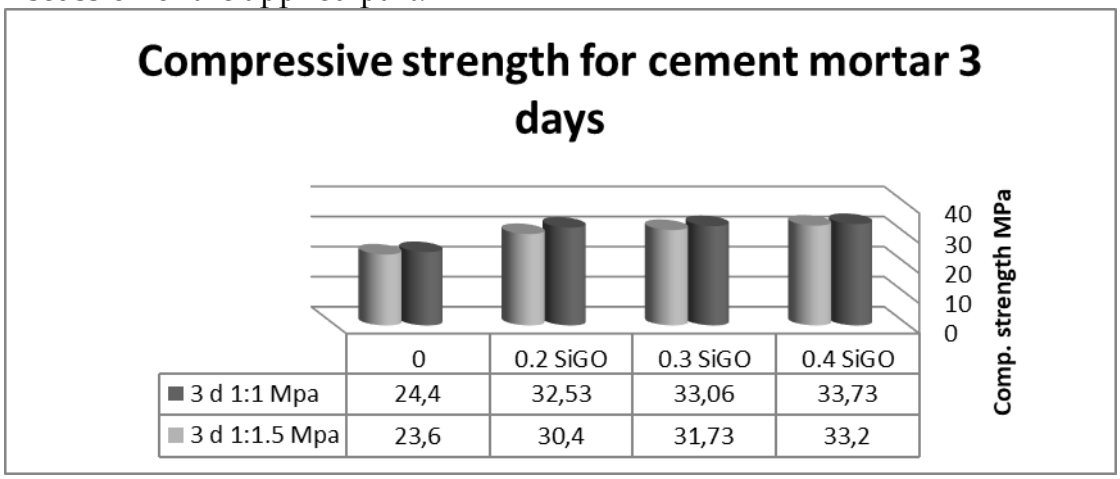

Figure 18. Compressive Strength for Cement Mortar 3 Days

Figure (3-1) represents the cement mortar values for Si GO composites with weights of 0.2, 0.3, and 0.4, and the reference mix. This ratio showed a higher compressive strength compared to the 1:1.5 ratio for the same composite, reaching 33.73 MPa at three days of age. The increase in compressive forte was concentrated with the addition of 0.4 g, followed by a decrease with 0.3 g and 0.2 g, respectively, as shown in Figure (3-70), which represents the cement mortar values for Si GO composites with weights of 0.2, 0.3, and 0.4, and the reference mix.

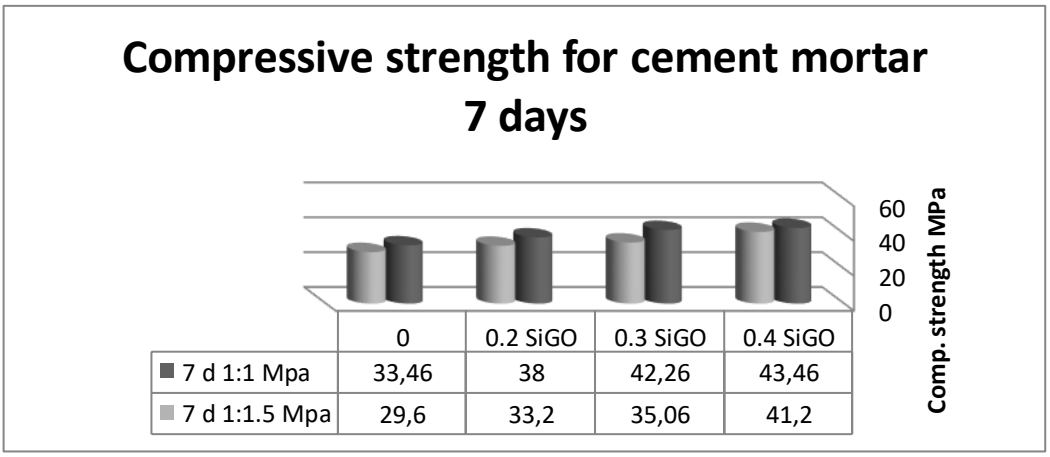

Figure 19. Compressive Strength for Cement Mortar 7 Days

Figure (3-8) represents the cement mortar values for the SiGO compound with weights of 0.2, 0.3, and 0.4 and the reference mix with an age of 7 days. The Si GO compound recorded the highest compressive strength for the same ratio of 43.46 MPa at the age of seven days. The increase in compressive forte was concentrated at the addition of 0.4 g, followed by a decrease at 0.3 g and 0.2 g, respectively.

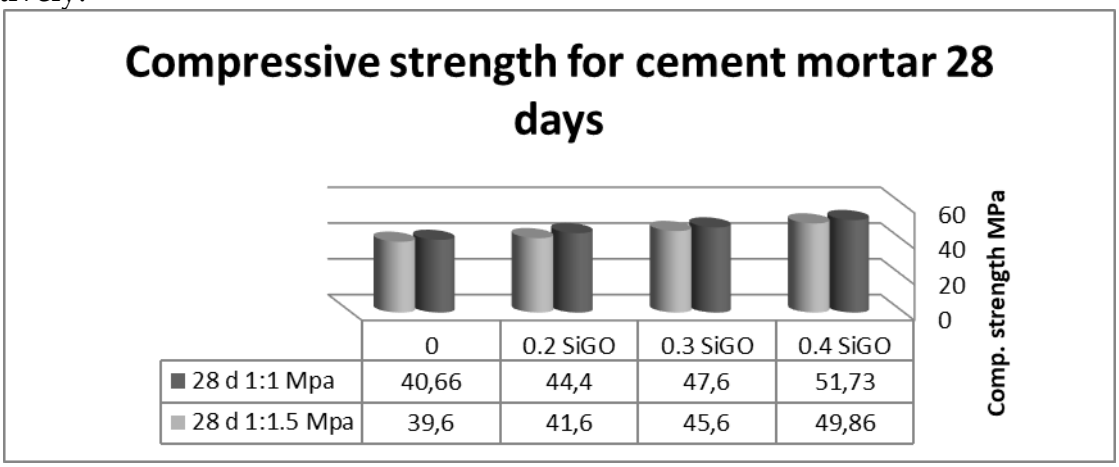

Figure 20. Compressive Strength for Cement Mortar 28 Days

Figure (3-14) shows the cement mortar values for the SiGO composite and the reference mix at 28 days of age.

A cement-to-sand ratio of 1:1 for the SiGO composite showed a higher compressive strength value compared to the 1:1.5 ratio for the same composite, reaching 51.73 MPa at 28 days of age. The increase in compressive forte was concentrated at the 0.4-gram addition, followed by a decrease at 0.3-gram

additions, recording a compressive strength of 47.6 MPa, and 0.2-gram additions, recording a compressive strength of 44.4 MPa, respectively.

CONCLUSIONS AND RECOMMENDATIONS

This study successfully developed a graphene oxide synthesis method using a modification of the Hummer method, which was then combined with silica-based phenolic compounds to produce graphene nano foil (Si GO) composites. The synthesis process showed effectiveness in producing nanostructures with appropriate morphological characteristics, crystallinity, and surface functional groups, as evidenced by FT-IR, UV-Vis, SEM, XRD, and AFM analyses. The use of this graphene-silica composite as an additive in cement mortar showed a significant increase in compressive strength, especially at a concentration of 0.4 grams, both at the ages of 3, 7, and 28 days. This shows that the composite has high application potential in the construction sector, especially to improve the mechanical performance of building materials.

1. Composite Concentration Optimization: Further research is recommended on the concentration range of graphene-silica composites to determine the optimal point of use in cement mixtures with a wider variation of cement-sand ratios.
2. Long-Term Durability Study: Further evaluation of the long-term durability of the modified cement mortar is needed, including resistance to water, extreme temperatures, and chemical attacks (such as sulphates or chloride).
3. Exploration of Other Applications: Given the multifunctional nature of graphene-silica composites, research can be extended to other applications such as anti-corrosion coatings, filtration materials, or electrode materials in energy devices.
4. Scalability and Production Efficiency: The efficiency and scalability of this synthesis method in an industrial context, especially related to aspects of cost, ease of replication, and environmental safety, is needed.

FURTHER STUDY

This research still has limitations so further research is still needed on this topic.

REFERENCES

Ansón-Casaos, A., et al. (2014). The effect of gamma-irradiation on few-layered graphene materials. Applied Surface Science, 301, 264-272.

Bernauer, U., et al. (2019). SCCS opinion on solubility of synthetic amorphous silica (SAS) - Final opinion and corrigendum.

Dalla, P. T., et al. (2021). Multifunctional cement mortars enhanced with graphene nanoplatelets and carbon nanotubes. Sensors, 21(3), 933.

De Silva, K. K. H., et al. (2017). Chemical reduction of graphene oxide using green reductants. Carbon, 119, 190-199.

Geim, A. K. (2009). Graphene: status and prospects. Science, 324(5934), 1530-1534.

Gong, K., et al. (2015). Reinforcing effects of graphene oxide on portland cement paste. Journal of Materials in Civil Engineering, 27(2), A4014010.

Hintze, C., et al. (2016). Facile sol–gel synthesis of reduced graphene oxide/silica nanocomposites. Journal of the European Ceramic Society, 36(12), 2923-2930.

Mohammed, Y. A. (2019). Synthesis and characterization of new polymer composite with nanoparticles. Research Journal of Pharmaceutical, Biological and Chemical Sciences.

Zaitseva, N., et al. (2016). Solid-phase spectrophotometric analysis of 1-naphthol using silica functionalized with m-diazophenylarsonic acid. Nanoscale Research Letters, 11(1), 1-8.

Zhu, Y., et al. (2010). Graphene and graphene oxide: synthesis, properties, and applications. Advanced Materials, 22(35), 3906-3924.